

1 **Local diagnostic of mixing and barrier modulation at**
2 **the tropopause**

Francesco d'Ovidio and Bernard Legras

3 Laboratoire de Météorologie Dynamique and CNRS, Ecole Normale

4 Supérieure, 24 rue Lhomond, F-75231 Paris, France.

5 (dovidio,legras@lmd.ens.fr)

Emily Shuckburgh

6 Centre for Atmospheric Science, Department of Applied Mathematics and

7 Theoretical Physics, University of Cambridge, Cambridge, CB3 0WA, UK.

8 (E.F.Shuckburgh@damtp.cam.ac.uk)

Francesco d'Ovidio & Bernard Legras, Laboratoire de Météorologie Dynamique, Ecole Normale Supérieure and CNRS, 24 rue Lhomond, F-75231 Paris, France (dovidio@lmd.ens.fr, legras@lmd.ens.fr)

Emily Shuckburgh, Centre for Atmospheric Science, Department of Applied Mathematics and Theoretical Physics, University of Cambridge, Cambridge, CB3 0WA, UK (E.F.Shuckburgh@damtp.cam.ac.uk)

9 Based on the assumption of a zonal structure for the large scale flow in
10 the UTLS, mixing barrier properties at the tropopause are often elucidated
11 by diagnostics based on zonal means. The lack of event resolution along the
12 longitude hinders such diagnostics in detecting local mixing events like bar-
13 rier breaks. For such events, their spatial localization is nevertheless the most
14 important feature affecting tracer distribution. Here we propose the deriva-
15 tion of a local diagnostic for mixing. The diagnostic combines forward Lya-
16 punov calculation (describing the stretching experienced by a tracer in the
17 future) with backward Lyapunov calculation (containing the information on
18 the tracer local gradient orientation due to the previous advection). The di-
19 agnostic is shown to be linearly correlated with the effective diffusivity in
20 zonal means, so that it can be expressed in diffusion units. As an example
21 of the application of this new diagnostic, we show the modulation of the sub-
22 tropical barrier in connection with ENSO focusing on local barrier breaks.

1. Introduction

23 It is now well established that the distribution of tracers in the upper troposphere and
24 the lower stratosphere (UTLS) depends on the transport and mixing properties of the
25 flow. It is also well accepted that the dominant, isentropic motion induces a chaotic type
26 of transport which, in turn, generates transport barriers within the flow and segregates
27 tracers into separated reservoirs. Motivated by the observation that these barriers are
28 along jets and that the segregation is mainly zonal, several diagnostics based on zonal
29 averages have been developed and applied to large wind datasets provided by analysis
30 and reanalysis from operational weather centers. Calculation of the stretching rates of
31 potential vorticity contours has been used to show that the edge of the polar vortex
32 corresponds to a minimum of this quantity [*Pierce and Fairlie, 1993; Scott et al., 2003*].
33 Effective diffusivity, introduced by *Nakamura [1996]* and applied to the UTLS by *Haynes*
34 *and Shuckburgh [2000a]* goes one step further by reducing the advection-diffusion of a
35 tracer on isentropic surface to pure diffusion, averaged in longitude in a new coordinate
36 system that follows the contours of the tracer. This approach bears the essential advantage
37 of providing a parametrization of turbulent transport across the tracer contours in terms
38 of a diffusion coefficient which measures quantitatively how leaky the barrier is.

39 Such approaches are however inevitably limited by their failure to represent some im-
40 portant longitudinal variations. Firstly, these calculations are implicitly assuming that
41 mixing, due to three-dimensional small-scale turbulent processes and eventually by molec-
42 ular forces, is preceded by the intensification of gradients on isentropic surfaces. Such
43 intensification occurs by a variety of mechanisms, like upper level frontogenesis at the

44 tropopause, but is essentially local in character with some preferred locations in longi-
45 tude where synoptic variability concentrates. Secondly, it is unclear whether barriers are
46 necessarily continuous in longitude and do not exhibit breaks at some locations – for
47 instance the average subtropical jet at the tropopause is not continuous all around the
48 globe. The investigation of such effects is clearly not amenable to methods where a single
49 value represents all mixing events along an entire contour.

50 The local Lyapunov exponent, either calculated for a finite time (FTLE) [*Pierrehumbert,*
51 1991; *Hu and Pierrehumbert, 2001*] or for a finite size (FSLE) [*Artale et al., 1997; Boffetta*
52 *et al., 2000*], measures the stretching of a small advected fluid element. It allows to
53 pinpoint transport properties very accurately in space and time, and is not limited, unlike
54 contour diagnostics, to two dimensions. Extrema of Lyapunov exponents have been used
55 to map coherent structures [*Haller and Yuan, 2000; Haller, 2001; Lapeyre, 2002*] and it
56 can be shown that lines of extrema often act as transport barriers [*Shadden et al., 2005*]
57 over a bounded range of times. However, the use of Lyapunov exponents for quantifying
58 mixing is based on a heuristic assumption and no quantitative relation with mixing has
59 been established so far to our knowledge.

60 Moreover there are fundamental problems with the interpretation of the results of Lyapunov
61 exponent calculations. In particular, climatologies of Lyapunov exponents may be
62 ambiguous to interpret. Low values indicate in general low mixing (either due to elliptic
63 structures or due to regions of weak chaotic stirring). However, transport barriers formed
64 by unstable manifolds of hyperbolic points and regions of strong chaotic mixing both
65 provide large exponents, but have an opposite effect on mixing

66 Local Lyapunov exponents and effective diffusivity have been compared, but only qual-
67 itatively. There is some confusion in the literature since the stretching of contours is often
68 taken as an estimate of the Lyapunov exponent. This is only true at asymptotically large
69 time but can be grossly incorrect at finite time. *Joseph and Legras* [2002] has shown
70 that both diagnostics provide approximately the same location of the transport barrier
71 surrounding the Antarctic polar vortex. In the case of an idealized incompressible, two-
72 dimensional, time-periodic flow with two regions separated by a barrier, *Shuckburgh and*
73 *Haynes* [2003] found that the two methods showed a minimum at the barrier for weak
74 mixing but that the minima in effective diffusivity was not reproduced by the Lyapunov
75 exponent for stronger mixing. Other (unpublished) attempts done by the authors based
76 on advection by analysed atmospheric winds at mid-latitude failed to show a correlation
77 between effective diffusivity and Lyapunov exponents.

78 This paper aims to bridge this gap in our understanding of the relation between mixing
79 and stretching by providing a new diagnostic with both advantages: parametrization of
80 mixing in diffusion units and detection of local events. We focus on a case study arising
81 in the UTLS region, although the method could be applicable to a range of geophysical
82 flows. We start by computing the Lyapunov exponents and the effective diffusivity on
83 the 350K isentropic level over an extended period. The direct comparison of the two
84 diagnostics shows the lack of any definitive correlation. However, theoretical arguments
85 suggest how to derive a new quantity based on the Lyapunov exponent (that we will
86 call the ‘transverse Lyapunov exponent’) which is linearly correlated with the effective
87 diffusivity. This correlation allows us to perform a linear fit that converts the units of

88 the Lyapunov diagnostic into those of a diffusivity. From a physical viewpoint, the fitting
89 procedure provides an estimate for a cutoff time for the local growth of a tracer contour.
90 This time sets the crossover between the contour expansion due to chaotic filamentation
91 and removal of thin filaments due to small-scale turbulence. The application of the TLE
92 to ENSO shows that indeed the diagnostic is able to quantify local phenomena such as
93 barrier breaks, and at the same time is in good quantitative agreement with the effective
94 diffusivity when zonally averaged.

2. Data and method

95 The calculations are performed on the 350K isentropic surface using the ERA-40 re-
96 analysed winds provided by the European Centre for Medium-Range Weather Forecasts
97 [Uppala, 2005] over the period 1980-2001. The choice of this period is dictated by the
98 relative homogeneity of the assimilated data, notably the satellite data provided by TOVS
99 instruments, cloud-wind products and surface data from buoys.

The effective diffusivity is obtained daily by analysing the contours of a test tracer evolving according to an advection-diffusion equation where advection is by the ERA-40 winds *Haynes and Shuckburgh* [2000a]. The calculation is performed by pseudo-spectral method using a T159 spherical harmonics representation and associated collocation grid. The tracer is initialized with a concentration proportional to the sine of the latitude. The contours are calculated after a "spin-up" time of one month used to get a result independent of the initial conditions. The equivalent contour length L_{eq} [*Haynes and Shuckburgh*, 2000a] is then calculated as a function of the equivalent latitude ϕ_e with spacing of approximately 1° . The effective diffusivity is related to the equivalent length

by :

$$\kappa_{\text{eff}} = \kappa_0 \frac{L_{\text{eq}}^2}{(2\pi r \cos \phi_e)^2}, \quad (1)$$

100 where r is the Earth radius. The parameter κ_0 is a constant diffusivity (taken as $1.5 \cdot 10^5$
 101 m^2/s^{-1}) used to parametrize diffusion due to small-scale turbulence. It has been show
 102 that the effective diffusivity is largely independent on the value of κ_0 (see *Haynes and*
 103 *Shuckburgh* [2000a] for a sensitivity study of the effect of κ over the effective diffusivity).

104 The FSLEs are computed on a quasi-regular latitude-longitude grid, with a 0.5° spacing
 105 in latitude. Winds from the ERA-40 spectral T159 representation are interpolated in time
 106 using cubic splines and bi-linearly in space from an intermediate projection to a 480×242
 107 Gaussian grid. Trajectories of Lagrangian parcels are constructed both forward and back-
 108 ward in time. At each grid-point, the trajectories starting at the four cardinal corners of
 109 a small square with a diagonal $\delta_0 = 0.1^\circ$ are followed, until a prescribed relative separation
 110 $\delta = 5\delta_0$ is reached for one of the diagonal. The exponents and the eigen-directions are
 111 obtained from the singular values and directions of the matrix that transforms the initial
 112 square into a parallelepiped [*Koh and Legras*, 2002]. Other details are as in *Mariotti et al.*
 113 [1997] and *Joseph and Legras* [2002].

3. A diagnostic for local events

The scatter plot of FSLEs and $\log(\kappa_{\text{eff}})$ monthly means (Fig. 1 a) exhibits a large spread which does not suggest any relation between the two quantities. As discussed in the introduction, this is not surprising since the stretching detected by the FSLE may correspond to either a transport barrier or to a region of vigorous chaotic mixing. Figure 2 shows that the Lyapunov exponent is maximum along the winter subtropical jet,

a region where the effective diffusivity is minimum. This anticorrelation arises because, within the jet, stretching is mainly due to shear that separates particle pairs but does not affect tracer contours if they are aligned with the shear. Since alignment of tracer contours with stretching axis is also a consequence of chaotic advection [*Klein et al.*, 2000; *Lapeyre et al.*, 2001], the two effects combine to inhibit the growth of tracer gradient and subsequent mixing. Technically, the eigendirections of the forward and backward leading Lyapunov vector tend to align within strong shear regions, as seen for instance in [*Joseph and Legras*, 2002, Fig.2]. With this mechanism in view, it is now possible to provide a corrected estimate of the tracer gradient growth. Assuming that at any time, the tracer gradient is orthogonal to the most unstable direction calculated from backward evolution, the tracer gradient growth is given by the *transverse Lyapunov exponent* (TLE) defined as

$$\lambda_{\perp} = \lambda_f |\sin(\varphi)|, \quad (2)$$

114 where λ_f is the leading forward Lyapunov exponent and φ is the angle between the local
 115 intersection of (forward) stable and (backward) unstable directions.

The TLE has values reduced by about a factor 2 with respect to the standard FSLE and shows now a clear correlation with the effective diffusivity (Fig. 1b). This suggests we try fitting the effective diffusivity to the TLE by defining a local *Lyapunov diffusivity* κ_{λ} such that $\ln \kappa_{\lambda}/\kappa_0 = A + B\lambda_{\perp}$, where A and B are provided by the fit. The dispersion of the scatter plot can be further reduced if A and B are calculated separately for each latitude strip (of 1°), resulting into a remarkably narrow linear relation shown in Fig. 3a. A physical interpretation of B is obtained by noting from (1) that the equivalent length

at each latitude scales like

$$L_{\text{eq}} \sim e^{\lambda_{\perp} T_{\kappa}(\phi)},$$

116 where $T_{\kappa}(\phi)$ is a characteristic time scale over which exponential growth by filamentation
 117 and turbulent diffusion by small-scale turbulence balance in a quasi-steady state for L_{eq} .
 118 Hence B provides an estimate of $T_{\kappa}(\phi)$ Figure 3b shows the latitudinal variations of
 119 $T_{\kappa}(\phi)$, indicating, that T_{κ} reaches a minimum of about 2 days near the equator while it is
 120 maximum near 20S and 20N (12 days and 20 days respectively). A secondary maximum
 121 is seen near 35S and 35N in both hemispheres.

4. Modulation of the subtropical barrier during El Niño

122 The previous section has demonstrated that zonally average TLE shows excellent agree-
 123 ment with effective diffusivity. We now turn to the main advantage of this new diagnostic
 124 to resolve the variability of mixing events in longitude. Figure 4a shows that during the
 125 boreal winter 1998-1999, the TLE is minimum over a large portion of the subtropical
 126 jet in the northern hemisphere. The zonally averaged κ_{λ} is plotted along with effective
 127 diffusivity on Fig. 5. Although the two curves show coinciding minima, only the TLE
 128 reveals the break in the barrier observed in the eastern Pacific on Fig. 4a. This particular
 129 winter was chosen because it corresponds to a weak negative phase of ENSO oscillation
 130 according to [Wolter and Timlin, 1998], but a global average over 22 winters (not shown)
 131 exhibits essentially the same pattern. In contrast, Fig. 4b shows that during the strong
 132 El Niño winter 1997-1998, the east Pacific break disappears and that except perhaps over
 133 the Atlantic, the subtropical jet exhibits an almost continuous barrier around the Earth.
 134 A deeper minimum at 30N is also seen on the zonal average (Fig. 5), both for effective

135 diffusivity and κ_λ , but this average does not reveal the origin of the variation. g The east
 136 Pacific break in the subtropical barrier corresponds closely to the active baroclinic zone
 137 associated with the Asian jet stream and the climatology of intrusions into the tropical
 138 upper troposphere *Waugh and Polvani* [2000]. The weak mixing associated with win-
 139 ter 1997-1998 agrees with the reduction of eddy fluxes of momentum and temperatures
 140 observed during the same period by [*Shapiro et al.*, 2001].

141 The variation induced by El Niño also includes weakening of the mixing zone over India
 142 and the Indian ocean, and an increase of mixing in the equatorial Pacific which can be
 143 related with easier propagation of cross-equatorial waves *Tomas and Webster* [1994].

5. Discussion

144 We have shown that unlike the standard Lyapunov exponent, the TLE provides a local
 145 direct estimate of mixing. Locality is defined in a Lagrangian way since the TLE is defined
 146 itself as a temporal average over a typical duration of 5 days and mixing properties are
 147 mapped at the initial location of the parcel being mixed.

148 The TLE is converted into a local diffusivity through a characteristic time scale T_κ
 149 which has been determined empirically by a fit to effective diffusivity. The rationale of
 150 this approach is the striking linearity of zonal means shown in Fig. 3a. An independent
 151 theory to determine the large variations of T_κ with latitude is still missing.

152 The comparison of Fig. 2 with Fig. 4 shows that maxima of λ_f are frequently turned
 153 into minima of λ_\perp , or in other words that the distribution of the angles between local
 154 stable and unstable directions is strongly peaked near zero where λ is large. In agreement
 155 with *Haynes and Shuckburgh* [2000b], in spite of weaker Rossby wave activity, the summer

156 hemisphere is better mixed than the winter hemisphere. A geometrical interpretation is
157 that chaotic tangles [*del Castillo-Negrete and Morrison, 1993; Joseph and Legras, 2002*]
158 are strongly suppressed in the vicinity of the jet during winter and that the eddies are more
159 efficient at mixing in summer because the angles between stable and unstable directions
160 are larger. This is consistent with the findings of [*Marshall et al., 2006*] and [*Haynes et al.,*
161 *2006*] who have demonstrated that effective diffusivity is much increased when the zonal
162 mean is removed from the flow.

163 One of the new results highlighted by the TLE diagnostic is that the reinforcement of
164 the subtropical barrier associated with El Niño (Fig.5) is strongly localized in the east
165 Pacific. We believe that the TLE and the Lyapunov diffusivity will prove to be a useful
166 diagnostic of local mixing and transport, not just at the tropopause but also for a broad
167 range of geophysical flows. It may be particularly useful for oceanographic problems where
168 longitudinal variations can be of great importance.

Acknowledgments

169 FO has been supported during this research by Ministère de l'Enseignement Supérieur
170 (France) and by a Marie-Curie fellowship [024717-DEMETRA].

References

171 Artale, V., G. Boffetta, A. Celani, M. Cencini, and A. Vulpiani (1997), Dispersion of
172 passive tracers in closed basins: beyond the diffusion coefficient, *Phys. Fluids*, *9*, 3162–
173 3171.

- 174 Boffetta, G., M. Celani, G. Lacorata, and A. Vulpiani (2000), Nonasymptotic properties
175 of transport and mixing, *Chaos*, *10*, 50–60.
- 176 del Castillo-Negrete, D., and D. Morrison (1993), Chaotic transport of Rossby waves in
177 shear flow, *Phys. Fluids A*, *5*(4), 948–965.
- 178 Haller, G. (2001), Lagrangian coherent structures and the rate of strain in two-dimensional
179 turbulence, *Phys. Fluids*, *13*, 3365–3385.
- 180 Haller, G., and G. Yuan (2000), Lagrangian coherent structures and mixing in two-
181 dimensional turbulence, *Physica D*, *147*, 352–370.
- 182 Haynes, P., and E. Shuckburgh (2000a), Effective diffusivity as a diagnostic of atmo-
183 spheric transport. Part I: stratosphere, *J. Geophys. Res.*, *105*(D18), 22,777–22,794,
184 doi:10.1029/2000JD900092.
- 185 Haynes, P., and E. Shuckburgh (2000b), Effective diffusivity as a diagnostic of atmospheric
186 transport. Part II: troposphere and lower stratosphere, *J. Geophys. Res.*, *105*(D18),
187 22,795–22,810, doi:10.1029/2000JD900092.
- 188 Haynes, P., D. Poet, and E. Shuckburgh (2006), Transport and mixing in kinematic and
189 dynamical-consistent flows, submitted to *J. Atmos. Sci.*
- 190 Hu, Y., and R. Pierrehumbert (2001), The advection-diffusion problem for stratospheric
191 flow. Part I: Concentration probability distribution, *J. Atmos. Sci.*, *58*, 1493–1510.
- 192 Joseph, B., and B. Legras (2002), Relation between kinematic boundaries, stirring, and
193 barriers for the Antarctic polar vortex, *J. Atmos. Sci.*, *59*, 1198–1212.
- 194 Klein, P., B. L. Hua, and G. Lapeyre (2000), Alignment of tracer gradient vectors in 2d
195 turbulence, *Physica D*, *146*, 246–260.

- 196 Koh, T.-Y., and B. Legras (2002), Hyperbolic lines and the stratospheric polar vortex,
197 *Chaos*, *12*(2), 382–394.
- 198 Lapeyre, G. (2002), Characterization of finite-time Lyapunov exponents and vectors in
199 two-dimensional turbulence, *Chaos*, *12*, 688–698.
- 200 Lapeyre, G., B. Hua, and P. Klein (2001), Dynamics of the orientation of active and
201 passive scalars in two-dimensional turbulence, *Phys. Fluids*, *13*, 251–264.
- 202 Mariotti, A., M. Moustou, B. Legras, and H. Teitelbaum (1997), Comparison between
203 vertical ozone soundings and reconstructed potential vorticity maps by contour advec-
204 tion with surgery, *J. Geophys. Res.*, *102*(D5), 6131–6142, doi:10.1029/96JD03509.
- 205 Marshall, J., E. Shuckburgh, E. Jones, and C. Hill (2006), Estimates and implications of
206 surface eddy diffusivity in the southern ocean derived from tracer transport, *J. Phys.*
207 *Ocean.*, *36*(9), 1806–1821.
- 208 Nakamura, N. (1996), Two-dimensional mixing, edge formation, and permeability diag-
209 nosed in an area coordinate, *J. Atmos. Sci.*, *53*(11), 1524–1537.
- 210 Pierce, R. B., and T. D. Fairlie (1993), Chaotic advection in the stratosphere: Implications
211 for the dispersal of chemically perturbed air from the polar vortex, *J. Geophys. Res.*,
212 *98D*(10), 18,589–18,595.
- 213 Pierrehumbert, R. (1991), Large-scale horizontal mixing in planetary atmospheres, *Phys.*
214 *Fluids A*, *3*(5), 1250–1260.
- 215 Scott, R. K., E. Shuckburgh, J.-P. Cammas, and B. Legras (2003), Effective diffusiv-
216 ity as a diagnostic of atmospheric transport, *J. Geophys. Res.*, *108*(D13), 4394, doi:
217 10.1029/2002JD002988.

- 218 Shadden, S. C., F. Lekien, and J. E. Marsden (2005), Definition and properties of La-
219 grangian structures from finite-time Lyapunov exponents in two-dimensional aperiodic
220 flows, *Physica D*, *212*, 271–304, doi:10.1016/j.physd.2005.10.007.
- 221 Shapiro, M., H. Wernli, N. Bond, and R. Langland (2001), The influence of the 1997-
222 1998 ENSO on extratropical baroclinic life cycles over the Eastern North Pacific,
223 *Quart. J. Roy. Met. Soc.*, *127*, 331–342.
- 224 Shuckburgh, E., and P. H. Haynes (2003), Diagnosing transport and mixing using a tracer-
225 based coordinate system, *Phys. Fluids*, *15*, 3342–3357.
- 226 Tomas, R., and P. Webster (1994), Horizontal and vertical structure of cross-equatorial
227 wave propagation, *J. Atmos. Sci.*, *51*(11), 1417–1430.
- 228 Uppala, S. *et al.* (2005), The ERA-40 re-analysis, *Quart. J. Roy. Met. Soc.*, *131*, 2961–
229 3012.
- 230 Waugh, D., and L. Polvani (2000), Climatology of intrusions into the tropical upper
231 troposphere, *Geophys. Res. Lett.*, *27*(23), 3857–3860.
- 232 Wolter, K., and M. S. Timlin (1998), Measuring the strength of ENSO - how does 1997/98
233 rank?, *Weather*, *53*, 315–324.

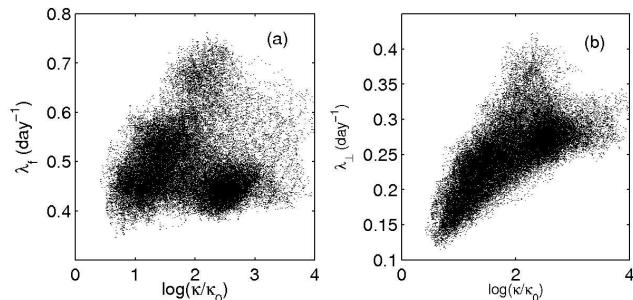


Figure 1. Scatter plots of monthly-means of zonally averaged forward (a) and transverse (b) Lyapunov exponents vs. effective diffusivity for the period 1980-2000 of the 350 K isentropic layer of the ERA-40 reanalysis.

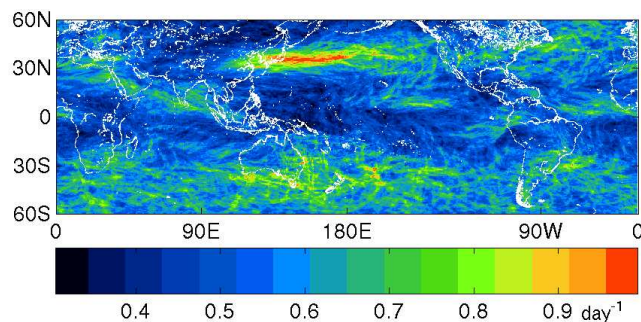


Figure 2. Forward Lyapunov exponent at 350K averaged over winter 1998-1999 (December-January).

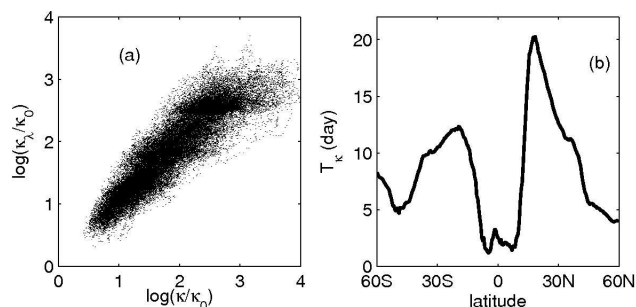


Figure 3. (a) Correlation between the effective diffusivity derived by a latitude-dependent linear fit of the transverse Lyapunov exponent and the effective diffusivity directed calculated. (b) Multiplicative coefficient of the linear fit T_{κ} .

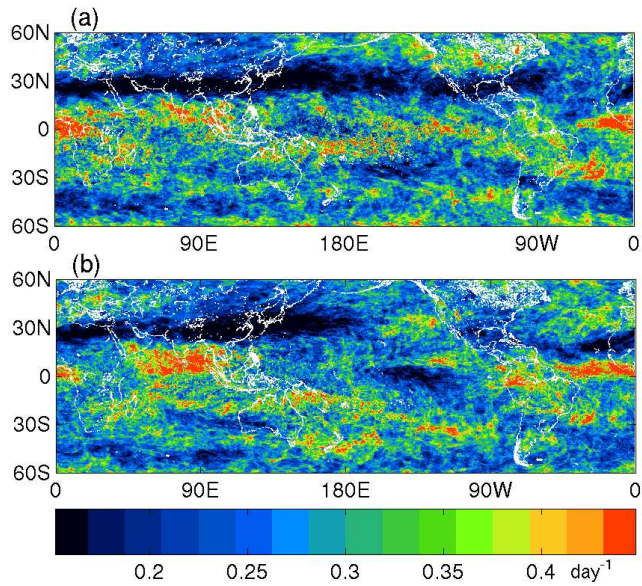


Figure 4. TLE during the La Niña winter 1998-1999 (top) and the El Niño winter 1997-1998 (bottom).

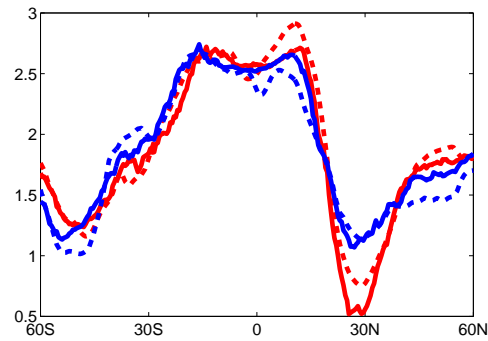


Figure 5. Zonally averaged Lyapunov diffusivity (continuous line) and effective diffusivity (dashed line) for the El Niño winter 1997-1998 (red) and La Niña winter 1998-1999 (blue).

